Mean-field theory of entropy-driven structural phase transitions

W. C. Kerr and M. J. Rave*
Olin Physical Laboratory, Wake Forest University, Winston-Salem, North Carolina 27109-7507
(Received 6 July 1993)

Models for lattice dynamical systems possessing first-order structural phase transitions have recently been constructed, and extensive molecular-dynamics calculations have been carried out for them. The mechanism producing the transition is that there are lower vibrational frequencies in the high-temperature structure than in the low-temperature structure, thereby increasing the entropy of the high-temperature phase. These structure-dependent frequencies are produced by anharmonicity in the interparticle interaction. This paper describes a mean-field theory for such entropy-driven transitions. It is based on making a Gaussian ansatz for the single-particle probability density function. Qualitatively, the results agree well with the molecular-dynamics simulations. We use the theory to make a more extensive survey of the parameter space than has been done with the simulations. We find that there are three different intervals for the strength of the anharmonicity, in each of which the high-temperature behavior of the order parameter is different in an important way. This change is a possible explanation for the hysteresis found in the simulations.

I. INTRODUCTION

The diversity of both the categories of phase transitions and the mechanisms for causing them continues to motivate further research. The category of structural phase transitions provides some of the most interesting examples and problems. The earliest theoretical understanding of *continuous* structural transitions came from Cochran's[1] and Anderson's[2] theory of the soft-mode mechanism, which was a mean-field theory. The experimental results on the continuous (second-order) transition in $SrTiO_3$ showed that in addition to the soft mode, there are additional features beyond those captured by mean-field theory. These include non-mean-field critical exponents,[3] and the existence of anomalous intense quasielastic intensity in the neutron-scattering spectrum[4] in a large temperature interval around the transition. This example showed that the continuous structural transitions are members of the universality classes identified by the renormalization-group analysis of critical phenomena.

Efforts to extend these ideas to their limit of applicability have produced the recognition that a far larger set of structural transitions are discontinuous (first-order) and have phonon frequencies which are only very weakly temperature dependent. The cannot be included in the soft-mode classification.[5–7] This realization led to a search for models possessing mechanisms which produce first-order structural transitions. One such model, which has been the subject of recent investigations, has an *entropy-driven* first-order transition. There are two versions of this model; the one we are concerned with in this paper has an asymmetric transition,[8] whereas the other has a symmetry-breaking transition.[9] These recent papers describe the motivation and construction of this model in detail and also present results of extensive molecular-dynamics (MD) calculations of its properties. The same physical idea has also been used recently to model the denaturation transition in DNA.[10]

Anharmonic forces are an essential feature of this model, for both the *single-particle* and *interparticle* forces. In models for second-order transitions (e.g., the "ϕ^4" model[11]), the on-site potential is a symmetric double well; this symmetry is spontaneously broken in the transition to the low-temperature phase. The model used here for first-order transitions has an *asymmetric* on-site potential, which eliminates the possibility for spontaneous symmetry breaking. This asymmetry pushes the particles toward the deeper minimum of the on-site potential, and thus acts like an external field, which usually prevents phase transitions. However, having anharmonicity also in the *interparticle* interactions introduces a competing factor. These anharmonic interactions are constructed to make the phonon frequencies structure dependent in such a way that the structure with the higher internal energy has lower frequencies. This mechanism increases the entropy associated with that structure. If the interparticle anharmonicity is sufficiently strong, then the structure with higher internal energy achieves lower *free energy* at higher temperatures, so that a phase transition to that structure occurs.

Our purpose in this paper is to develop a mean-field theory (MFT) for this model. We know that MFT does not describe the details of phase transitions quantitatively accurately. However, a comprehensive theory for first-order transitions, comparable to the renormalization group for second-order transitions, does not exist. Furthermore, the resource-intensive nature of MD calculations means that method can be used to study only a few values in the parameter space of the system. For these reasons, it is desirable to have a means to make an extensive, albeit approximate, survey of the properties of the system throughout its parameter space.

The particular MFT developed here is a modification and extension of a theory introduced by Thomas[12,13] to analyze second-order structural transitions, like that ex-

hibited by $SrTiO_3$. The fundamental hypothesis is that the single-particle probability distribution for the displacements is a Gaussian function. From that assumption a theory can be constructed which agrees qualitatively with the MD simulations for those sets of parameter values where the simulations have been done and which extends throughout the parameter space.

The outline of this paper is as follows. Section II describes the model. Section III derives the MFT equations. Section IV analyzes the MFT equations for the case of no interparticle anharmonicity, showing the relation of the present theory with other models. Section V then gives the solution with the interparticle anharmonicity included, which is the focus of this paper. Section VI gives our conclusions.

II. THE MODEL

The model is the same as was used for the computer simulations of Ref. 8; it is defined by the Hamiltonian

$$H=\sum_{\mathbf{n}} \tfrac{1}{2}p_{\mathbf{n}}^2+\sum_{\mathbf{n}} V_1(u_{\mathbf{n}})+\tfrac{1}{2}\sum_{\mathbf{n},\delta} V_2(u_{\mathbf{n}},u_{\mathbf{n}+\delta}) . \tag{1}$$

Here $\mathbf{n}$ denotes the sites of a D-dimensional hypercubic lattice, δ denotes the set of nearest-neighbor lattice vectors, and $u_{\mathbf{n}}$ is a scalar displacement variable at the $\mathbf{n}$th lattice site. The on-site potential energy $V_1(u)$ is an asymmetric function of the displacement (Fig. 1)

$$V_1(u)=\tfrac{1}{2}a_0u^2-\tfrac{1}{3}u^3+\tfrac{1}{4}u^4 . \tag{2}$$

(All quantities in this paper have been scaled to dimensionless values to eliminate nonessential factors. The scaling is the same as that employed by Krumhansl and Gooding;[6] it is explained in detail in Ref. 8, and the scaling factors are given in Table II of that paper.) For $a_0=\frac{2}{9}$, $V_1(u)$ is a symmetric double-well potential with degenerate minima at $u=0$ and $\frac{2}{3}$ and a maximum at $u=\frac{1}{3}$. For $0<a_0<\frac{2}{9}$, it has a metastable minimum at $u=0$, a maximum at $u_{\max}$, and a stable minimum at $u_{\min}$,

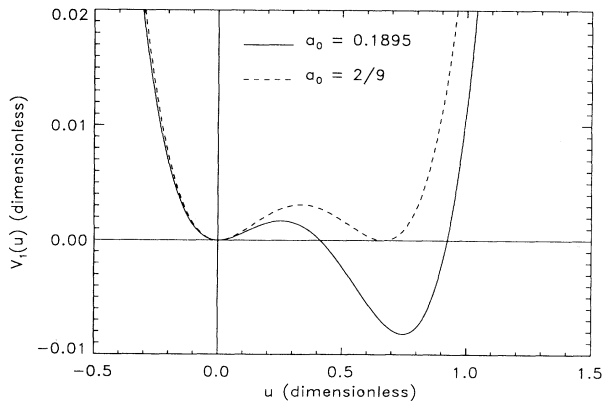

FIG. 1. The on-site potential function of Eq. (2). The dashed curve is for $a_0=\frac{2}{9}$ and is symmetric about $u=\frac{1}{3}$. The solid curve is for $a_0=0.1895$, the value used for the simulations in Ref. 8.

which are given by

$$u_{\max}=\tfrac{1}{2}[1-\sqrt{1-4a_0}]<\tfrac{1}{3} ,$$
$$u_{\min}=\tfrac{1}{2}[1+\sqrt{1-4a_0}]>\tfrac{2}{3} . \tag{3}$$

For later comparisons, we note that the asymmetric on-site potential in Eq. (2) can be written

$$V_1(u)=\tfrac{1}{4}[(u-\tfrac{1}{3})^2-\tfrac{1}{9}]^2 -(\tfrac{2}{9}-a_0)[\tfrac{1}{2}(u-\tfrac{1}{3})^2+\tfrac{1}{3}(u-\tfrac{1}{3})+\tfrac{1}{18}] . \tag{4}$$

The first term here is the symmetric potential (the "ϕ^4" potential), but with the coordinate origin at the left-hand minimum instead of at the maximum, as it is usually written. The rest of Eq. (4) shows the perturbations added when a_0 deviates from $\frac{2}{9}$; the only one which actually breaks the symmetry about $u=\frac{1}{3}$ is a linear term.

For the pair interaction potential energy we use

$$V_2(u,u')=\tfrac{1}{2}[k+\alpha(u+u')](u-u')^2 , \tag{5}$$

as was used in Ref. 8; the motivation for this choice is discussed at length in that paper. Gooding and Morris[9] have developed a theory based on the same ideas for symmetry-breaking transitions. The transition studied here is asymmetric.

With both the on-site potential taken to be symmetric ($a_0=\frac{2}{9}$) and the pair potential $V_2(u,u')$ in Eq. (5) taken to be a *harmonic* interaction, i.e., $\alpha=0$, then the model defined by Eqs. (2) and (5) is the much-studied ϕ^4 model.[11] In the displacive limit ($k\gg\frac{1}{18}$, in our dimensionless units), which justifies a continuum approximation, the model is known to have a second-order transition for dimensions $D\geq 2$. If the symmetry of the on-site potential is removed ($0<a_0<\frac{2}{9}$), but the interparticle potential is kept harmonic ($\alpha=0$), then the computer simulations showed that *no* phase transition occurs. Our MFT gives insight into that result (cf. Sec. IV). An argument due to Zener[14] provides guidance in modifying the model to obtain a first-order transition. One mechanism for stabilizing a higher-energy structure at nonzero temperature is for that structure to have a higher vibrational entropy, thereby realizing a lower free energy. Higher vibrational entropy results from having lower phonon frequencies in the high-temperature phase, and this effect can be achieved by introducing anharmonic interparticle forces in the way indicated in Eq. (5).

The MD simulations have shown, and the theory presented here also shows, that singularities appear in the thermodynamic functions of this system at a critical temperature T_c. Because of the asymmetry of the on-site potential, there is no breaking of symmetry, analogously to the liquid-gas transition, and there is only one variant of the low-temperature phase. There is only one kind of domain wall, between ordered and disordered regions of the system. A symmetry-breaking first-order transition, as presented in, e.g., Ref. 9, can also have "antiphase" domain walls, separating different variants of the low-temperature phase. The model used here may be the minimal *microscopic* model for a lattice-dynamical system possessing a first-order transition. However, phenomeno-

logical Landau free-energy functions have previously been constructed for non-symmetry-breaking first-order structural transitions.[6,15]

III. MEAN-FIELD THEORY

Mean-field theory assumes that the particles move independently, so that the phase-space distribution function factors into single-particle functions,[16]

$$F_N(\{p_n,u_n\})=\prod_n F_1(p_n,u_n) . \tag{6}$$

In classical statistical mechanics the momentum dependence is the Maxwell-Boltzmann function, so the single-particle distribution function has the form

$$F_1(p,u)=\frac{e^{-p^2/2T}}{\sqrt{2\pi T}}P_1(u) , \tag{7}$$

where T is the (dimensionless) temperature and $P_1(u)$ is the single-particle displacement distribution function. An immediate consequence is that the average kinetic energy is

$$\left\langle \sum_n \frac{p_n^2}{2} \right\rangle = \tfrac{1}{2}NT \tag{8}$$

(N is the total particle number). For the single-particle distribution function, we make an ansatz originally used by Thomas,[12,13] that this function is Gaussian with two parameters,

$$P_1(u)=\frac{1}{\sqrt{2\pi\sigma}}e^{-(u-u_0)^2/2\sigma} . \tag{9}$$

The two parameters in this function are the average displacement, which is related to the order parameter

$$\langle u \rangle \equiv \int_{-\infty}^{\infty} du\, uP_1(u)=u_0 , \tag{10}$$

and its mean-square fluctuation

$$\langle (u-u_0)^2 \rangle \equiv \int_{-\infty}^{\infty} du(u-u_0)^2P_1(u)=\sigma . \tag{11}$$

We note, for future use, that σ must be positive. For a Gaussian distribution, averages of other even powers of the fluctuation are related to the mean-square fluctuation, e.g.,

$$\langle (u-u_0)^4 \rangle = 3\sigma^2 , \tag{12}$$

and averages of odd powers of the fluctuation are zero.

Some justification for adopting this ansatz is provided by the computer-simulation results,[17] which calculated the single-particle probability distribution function for a small number of different parameter sets. For all cases the distributions were found to have a single maximum and to be very symmetric about that maximum, even close to the transition. A sensitive test of closeness to the Gaussian form is provided by calculating the ratio of the fourth moment to the square of the second moment. In the worst case the distributions from the simulations give values for this ratio which deviate by about 30% from the Gaussian value of three, due to extra weight in the wings. If we take this single maximum feature from the simulations as our assumption, further simplify it by taking the shape of the distribution to be Gaussian, and assume it to hold for all parameter values, then we can explain other features found in the simulations. Of course, it would be preferable to have an *a priori* justification of this assumption. In a subsequent paper[18] we will present a different approach in which the distribution function is a calculated result rather than an assumed input. The resulting distributions are not exactly Gaussian, but the deviations are similar in magnitude to the deviations seen in the simulations. This result then provides additional justification for continuing with this simpler Gaussian ansatz from which nearly all quantities can be obtained analytically.

The average of the on-site potential is

$$\begin{aligned}\left\langle \sum_n V_1(u_n) \right\rangle &= N[(\tfrac{1}{2}a_0u_0^2-\tfrac{1}{3}u_0^3+\tfrac{1}{4}u_0^4) \\ &\quad +\tfrac{1}{2}(a_0-2u_0+3u_0^2)\sigma+\tfrac{3}{4}\sigma^2] \\ &= N[V_1(u_0)+\tfrac{1}{2}V_1''(u_0)\sigma \\ &\quad +\tfrac{1}{24}V_1''''(u_0)\cdot 3\sigma^2] ,\end{aligned} \tag{13}$$

where the prime denote derivatives, and the second line just rewrites the previous expression in terms of the on-site potential energy. To compute the average of the interaction energy, we first express it in terms of single-particle terms and "irreducible" pair terms, so that the average of one pair interaction is

$$\begin{aligned}\langle V_2(u_n,u_{n+\delta}) \rangle &= \tfrac{1}{2}k[\langle u_n^2 \rangle+\langle u_{n+\delta}^2 \rangle-2\langle u_nu_{n+\delta} \rangle] \\ &\quad +\tfrac{1}{2}\alpha[\langle u_n^3 \rangle+\langle u_{n+\delta}^3 \rangle-\langle u_n^2u_{n+\delta} \rangle \\ &\quad -\langle u_nu_{n+\delta}^2 \rangle] .\end{aligned} \tag{14}$$

Then, by use of Eq. (9), the averages of the single-particle factors are

$$\begin{aligned}\langle u_n^2 \rangle &= \langle u_{n+\delta}^2 \rangle = u_0^2+\sigma , \\ \langle u_n^3 \rangle &= \langle u_{n+\delta}^3 \rangle = u_0^3+3u_0\sigma ,\end{aligned} \tag{15}$$

and because of the assumed factorization of the many-particle distribution function in Eq. (6),

$$\begin{aligned}\langle u_nu_{n+\delta} \rangle &= \langle u_n \rangle\langle u_{n+\delta} \rangle = u_0^2 , \\ \langle u_n^2u_{n+\delta} \rangle &= \langle u_n^2 \rangle\langle u_{n+\delta} \rangle = (u_0^2+\sigma)u_0 ,\end{aligned} \tag{16}$$

and similarly for $\langle u_nu_{n+\delta}^2 \rangle$. Thus,

$$\frac{1}{2}\left\langle \sum_{n,\delta} V_2(u_n,u_{n+\delta}) \right\rangle = N\tfrac{1}{2}(2D)(k+2\alpha u_0)\sigma , \tag{17}$$

where we have used the fact that there are $2D$ nearest-neighbor lattice vectors in a D-dimensional hypercubic lattice. We add Eqs. (8), (13), and (17) to get the internal energy per particle $u=\langle H \rangle /N$.

Next we calculate the entropy per particle from

$$s=-\frac{1}{N}\langle \ln F_N \rangle . \tag{18}$$

From the assumed distribution function in Eqs. (6), (7), and (9),

$$s=-\frac{1}{N}\sum_{n}\left[-\frac{1}{T}\langle\tfrac{1}{2}p_n^2\rangle-\tfrac{1}{2}\ln(2\pi T)-\frac{1}{2\sigma}\langle(u_n-u_0)^2\rangle-\tfrac{1}{2}\ln(2\pi\sigma)\right]$$
$$=1+\tfrac{1}{2}\ln(2\pi T)+\tfrac{1}{2}\ln(2\pi\sigma)\ . \tag{19}$$

The entropy is determined by the spread of the distribution function in the momentum and configuration spaces. The free energy per particle, $f=u-Ts$, is

$$f=(\tfrac{1}{2}a_0u_0^2-\tfrac{1}{3}u_0^3+\tfrac{1}{4}u_0^4)+\tfrac{1}{2}(a_0-2u_0+3u_0^2)\sigma+\tfrac{3}{4}\sigma^2+D(k+2\alpha u_0)\sigma-\tfrac{1}{2}T\ln(2\pi\sigma)-\tfrac{1}{2}T-\tfrac{1}{2}T\ln(2\pi T)\ . \tag{20}$$

The equilibrium values of u_0 and σ minimize the free energy f. They are the solution of the following MFT equations:

$$\frac{\partial f}{\partial u_0}=(a_0u_0-u_0^2+u_0^3)+(3u_0-1+2D\alpha)\sigma=0\ , \tag{21}$$

$$\frac{\partial f}{\partial\sigma}=\tfrac{1}{2}(a_0-2u_0+3u_0^2)+D(k+2\alpha u_0)+\tfrac{3}{2}\sigma-\frac{T}{2\sigma}=0\ . \tag{22}$$

The solutions of Eqs. (21) and (22) along with Eq. (20) for the free energy constitute the MFT description of the statistical mechanics of this system.

As an introduction to the analysis of these equations, we check the $T=0$ limit. Equation (22) shows that in the limit $T\to0$, the ratio T/σ remains finite, so it must be that $\sigma\to0$ also. This is the reasonable result that there are no fluctuations about the equilibrium position at zero temperature. Equation (21) reduces to

$$V_1'(u_0)\equiv(a_0u_0-u_0^2+u_0^3)=0\ . \tag{23}$$

This condition states that at $T=0$ the average position is one of the positions of mechanical equilibrium of the on-site potential, which are the positions $u_0=0$, and $u_{\max}$ and $u_{\min}$ of Eq. (3). Then from Eq. (20), since the $T\to0$ limit of both logarithmic terms is zero, the free energy is

$$f(T=0)=\tfrac{1}{2}a_0u_0^2-\tfrac{1}{3}u_0^3+\tfrac{1}{4}u_0^4\equiv V_1(u_0)\ . \tag{24}$$

Of the three possibilities for u_0, the stable equilibrium configuration is the absolute minimum of the on-site potential, which is the position $u_{\min}$ [see Fig. 1 and Eq. (3)].

IV. NO INTERPARTICLE ANHARMONICITY

In this section we analyze the solutions of the MFT equations for the $\alpha=0$ case. There are two subcases of interest here: (a) $a_0=\frac{2}{9}$, for which the on-site potential is symmetric about $u=\frac{1}{3}$ (dotted curve in Fig. 1), and (b) $a_0<\frac{2}{9}$, for which it is asymmetric (solid curve in Fig. 1).

A. $a_0=\frac{2}{9}$

For this case, the two MFT equations are

$$(u_0-\tfrac{1}{3})[u_0(u_0-\tfrac{2}{3})+3\sigma]=0\ , \tag{25}$$

$$(\tfrac{2}{9}-2u_0+3u_0^2)\sigma+2Dk\sigma+3\sigma^2=T\ . \tag{26}$$

There are two solutions to these equations. The simpler one is

$$u_0=\tfrac{1}{3} \tag{27}$$

from Eq. (25), for all T. The corresponding solution for σ is obtained by substituting Eq. (27) into Eq. (26); the physical (positive) solution is[19]

$$\sigma=\tfrac{1}{2}[-(\tfrac{2}{3}Dk-\tfrac{1}{27})+\sqrt{(\tfrac{2}{3}Dk-\tfrac{1}{27})^2+\tfrac{4}{3}T}\ ]\ . \tag{28}$$

The other solution of Eq. (25) is

$$\sigma=\tfrac{1}{3}u_0(\tfrac{2}{3}-u_0)\ . \tag{29}$$

We substitute this into Eq. (26) and obtain the T dependence of the average displacement. After some manipulations the result can be written

$$T=\tfrac{2}{3}[\tfrac{1}{9}-(u_0-\tfrac{1}{3})^2][(u_0-\tfrac{1}{3})^2+Dk\ ]\ , \tag{30}$$

which shows the symmetry about the line $u_0=\frac{1}{3}$. This equation can be rewritten as a quadratic equation in the quantity $(u_0-\frac{1}{3})^2$ and solved. Then we find a different character of the solution depending on the sign of $(Dk-\frac{1}{9})$. The computer simulations[8] were done for a *displacive* system, i.e., for larger force constants k, so we investigate that case first.

(a) $Dk>\frac{1}{9}$. In this case Eq. (30) can be inverted to

$$(u_0-\tfrac{1}{3})^2=\frac{3[\frac{2}{27}Dk-T]}{\sqrt{(Dk+\frac{1}{9})^2-6T}+(Dk-\frac{1}{9})}\ . \tag{31}$$

This equation shows that the order parameter $(u_0-\frac{1}{3})$ vanishes continuously at the mean-field critical temperature

$$T_c=\tfrac{2}{27}Dk\ , \tag{32}$$

and gives the canonical mean-field value $\beta=\frac{1}{2}$ for the order-parameter critical exponent. Figure 2 shows both solutions for u_0 vs T for this case. The parameter values used for the graph are the same as those used for the simulations in Ref. 8. Next we substitute the values of u_0 and σ for these two solutions into Eq. (20) for the free energy; the results are shown in Fig. 3. For $T<T_c$, the solution with the nonzero order parameter has the lower free energy. It joins continuously to the other solution at T_c, with continuous first-derivative (entropy) and discontinuous second-derivative (specific heat).

There are no MD calculations for this situation (symmetric on-site potential, isotropic harmonic force constants). However, there are simulations with *anisotropic* harmonic force constants.[20] For a system with uniaxial anisotropy, the MFT transition temperature of Eq. (32) changes to

$$T_c=\tfrac{2}{27}[k_\parallel+(D-1)k_\perp]\ . \tag{33}$$

Evaluated for the parameters of Ref. 20 this is $T_c^{(\mathrm{MFT})}=0.032$; from the simulations $T_c^{(\mathrm{MD})}\approx0.0185$.[21]

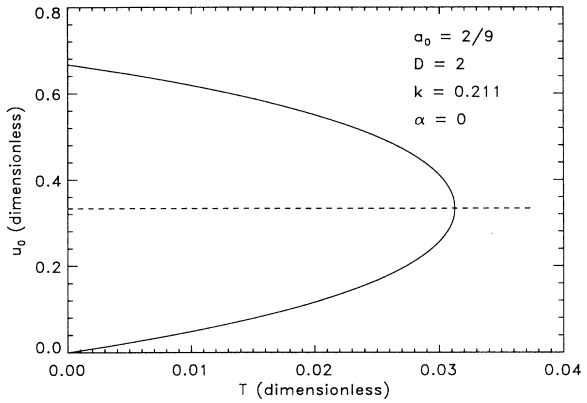

FIG. 2. Average displacement vs temperature for the case of the symmetric on-site potential and for a value of k in the displacive range, showing a second-order transition. The solid curve is the stable solution, Eq. (30). The dashed line is the unstable solution below T_c, and the only solution above T_c, Eq. (27).

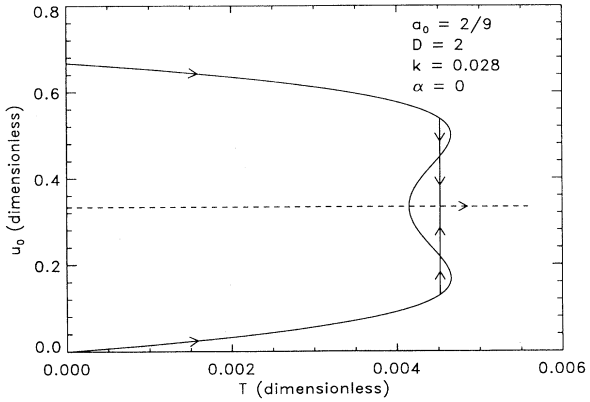

FIG. 4. Average displacement vs temperature for the case of the symmetric on-site potential and for a smaller value of k in the order-disorder range, showing a first-order transition. The solid curve is Eq. (30), and the dashed line is Eq. (27). The vertical line shows the transition temperature, as determined from equality of free energies of the two solutions. The arrows on the curves show the two possible paths followed by u_0 for increasing T, starting from $T=0$. The same paths are followed in the opposite direction for decreasing T.

As expected, MFT overestimates the transition temperature.

(b) $Dk < \frac{1}{9}$. For sufficiently weak interparticle force constants k, Eq. (30) predicts a multi-valued average displacement vs temperature relation, shown in Fig. 4. In this situation, the system jumps between the two solutions [Eqs. (27) and (30)] at the temperature where the free energies obtained from these two solutions become equal. The transition temperature for the particular k value used for the plot is $T_c \approx 0.004\,52\ldots$. The vertical line on the average displacement graph (Fig. 4) is drawn at this temperature. Thus, this theory predicts a *first-order transition* for sufficiently weak interparticle harmonic force constants. At the force constant value where the change from second-order to first-order behavior occurs, $Dk = \frac{1}{9}$, this theory predicts that the order-parameter critical exponent changes to $\beta = \frac{1}{4}$, which is the value for a tricritical point.[22]

On more general grounds we expect a crossover from displacive behavior for larger force constant values to order-disorder behavior for smaller values. The major distinguishing characteristic of order-disorder systems is that the single-particle probability distribution is *double peaked* in the low-temperature phase.[23] Since the theory of this paper is based on the assumption of a single-peaked (Gaussian) distribution, this prediction of a first-order transition should probably not be believed literally. One should rather take this to mean that a major change in behavior occurs for weak-coupling forces, and search for another approach to that case with less restrictive assumptions.

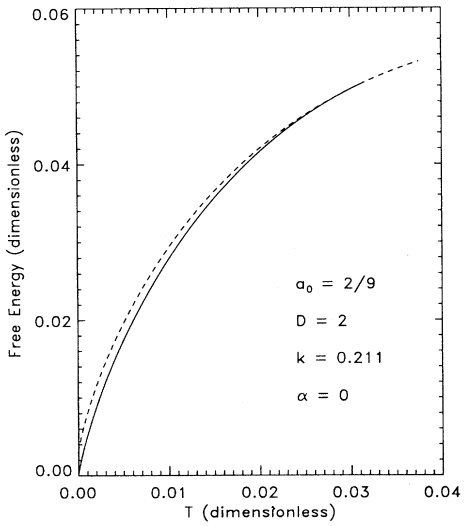

FIG. 3. The free energy vs temperature, from Eq. (20), corresponding to the average displacement curves in Fig. 2. The solid curve is for the stable solution and the dashed curve for the solution which is unstable below T_c and the only solution above T_c.

B. $a_0 < \frac{2}{9}$

For this case of the *asymmetric* on-site potential energy, we return to Eqs. (21) and (22) (still with $\alpha=0$). We solve Eq. (21) for σ:

$$\sigma = -\frac{a_0 u_0 - u_0^2 + u_0^3}{3(u_0 - \frac{1}{3})} = -\frac{1}{3}\frac{V_1'(u_0)}{u_0 - \frac{1}{3}} . \tag{34}$$

It is important to note here that Eq. (34) gives unphysical (negative) values for σ when u_0 is in the range $u_{\max} < u_0 < \frac{1}{3}$, where $u_{\max}$ is the location of the maximum of $V_1(u)$ [Eq. (3)] and therefore of a zero of $V_1'(u_0)$. We substitute this result for σ into Eq. (22) and obtain the relation between temperature and average displacement. After some manipulation this can be put in the form

$$T=\frac{1}{3}\left[\frac{1}{3}\frac{\frac{2}{9}-a_0}{u_0-\frac{1}{3}}+(\tfrac{1}{3}-a_0)-(u_0-\tfrac{1}{3})^2\right]\times\left[\frac{1}{3}\frac{\frac{2}{9}-a_0}{u_0-\frac{1}{3}}+2Dk+2(u_0-\tfrac{1}{3})^2\right] . \quad (35)$$

This way of writing the equation emphasizes that $T(u_0)$ for this case is a *rational function,* in contrast to the case $a_0=\frac{2}{9}$, where it is a *polynomial* [Eq. (30)]. Equation (35) shows that an infinitesimal deviation of a_0 from $\frac{2}{9}$ changes the analytic character of this function, so such a change in parameter value is a *singular perturbation.*

Figure 5 shows this average displacement vs temperature relation, plotted with T on the abscissa as is customary. The dashed part of the curve is unphysical both because σ is negative for that range of u_0 values and because T is negative over part of the range. Note that the high-temperature limiting value for the average displacement u_0 is $\frac{1}{3}$; this is the position of the maximum of the on-site potential for the *symmetric* case ($a_0=\frac{2}{9}$), but is not an extremum for the asymmetric case ($a_0<\frac{2}{9}$). The infinite temperature limit is still sensitive to the double well of the on-site potential, but not to the asymmetry of the two wells.

Figure 6 shows the free energy vs T for the two parts of the order-parameter curve. The solution with lower free energy comes from the top branch of the u_0 vs T relation. Both u_0 on this branch and the free energy are smooth functions, showing that *no* phase transition occurs. Making the on-site potential asymmetric has removed the transition that occurs for the symmetric double-well on-site potential. The MD simulations are in agreement with this result.

The way of writing the asymmetric on-site potential in Eq. (4) as the symmetric potential plus perturbations shows that one of the added terms is a linear function of the displacements. An external field would add a similar linear term, and external fields destroy phase transitions. That is evidently the reason why there is no phase transition in this case.

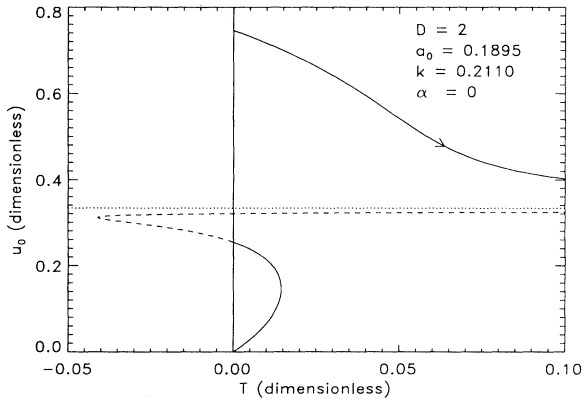

FIG. 5. Average displacement vs temperature for the asymmetric on-site potential but no interparticle anharmonicity ($\alpha=0$), Eq. (35). The dashed part shows the unphysical region where the width function σ [Eq. (34)] is negative, and also where Eq. (35) gives a negative T. The dotted line is the high-temperature asymptote, $u_0=\frac{1}{3}$. The arrow shows the path followed by u_0 for increasing T, starting from $T=0$.

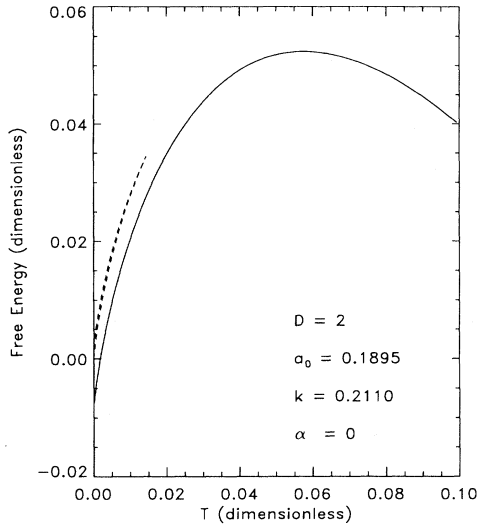

FIG. 6. The free energy vs temperature for the solutions shown in Fig. 5. The solid curve corresponds to the upper branch of Fig. 5, and the dashed curve is a very narrow loop corresponding to the lower branch. The two intercepts of the dashed curve with the $T=0$ axis are at the values $V_1(0)=0$ and $V_1(u_{\max})=0.002\,78$ [see Eq. (24)].

V. WITH INTERPARTICLE ANHARMONICITY

In this section we present the situation of major interest in this paper, which is the effect of anharmonicity in the interparticle interactions. We analyze the solutions of the full MFT equations, Eqs. (21) and (22), keeping the terms proportional to the anharmonicity parameter α.

The solution of Eq. (21) for the width function is

$$\sigma=-\frac{1}{3}\frac{V_1'(u_0)}{u_0-\frac{1}{3}(1-2D\alpha)} , \quad (36)$$

where $V_1'(u_0)$ is the first derivative of the on-site potential in Eq. (2). Substituting Eq. (36) into Eq. (22), we obtain the relation between temperature and average displacement for this case,

$$T=-\tfrac{1}{3}\frac{V_1'(u_0)}{[u_0-\frac{1}{3}(1-2D\alpha)]^2}\times\{[V_1''(u_0)+2D(k+2\alpha u_0)][u_0-\tfrac{1}{3}(1-2D\alpha)]-V_1'(u_0)\} . \quad (37)$$

The denominator in Eqs. (36) and (37) has a zero at

$$u_\infty(\alpha)=\tfrac{1}{3}(1-2D\alpha) . \quad (38)$$

This quantity is the high-temperature limit of the order parameter, i.e., the horizontal asymptote in the u_0 vs T relation. This high-temperature limit decreases from the value $u_\infty(\alpha=0)=\frac{1}{3}$, shown in Fig. 5, as α increases from

zero. The $V_1'(u_0)$ factor in the numerator of Eqs. (36) and (37) can be written

$$V_1'(u_0)=u_0(u_0-u_{\max})(u_0-u_{\min}) , \tag{39}$$

where $u_{\max}$ and $u_{\min}$ are defined in Eq. (3). The two zeros at $u_0=0$ and $u_0=u_{\max}$ are both less than $\frac{1}{3}$ (the third at $u_{\min}$ is larger than $\frac{2}{3}$ and so is not relevant here for $\alpha>0$). The zeros of $V_1'(u_0)$ are independent of α, so as α increases, the zero of the denominator of Eq. (37) at $u_0=u_\infty(\alpha)$ moves downward through the zeros of the numerator at $u_0=u_{\max}$ and at 0. At these switches in the ordering of the zeros of the numerator and denominator, the shape of the u_0 vs T relation in Eq. (37) changes. These switches occur at the α values where $u_\infty(\alpha)=u_{\max}$, which is

$$\alpha_{s1}=\frac{1}{4D}\left[3\sqrt{1-4a_0}-1\right] , \tag{40}$$

and where $u_\infty(\alpha)=0$, which is

$$\alpha_{s2}=\frac{1}{2D} . \tag{41}$$

For the D and a_0 values used in the MD calculations,[8] $\alpha_{s1}=0.0594\ldots$, and $\alpha_{s2}=0.25$. The properties of the solution change depending on the α value, so we present three cases separately.

A. $0<\alpha<\alpha_{s1}$ or $u_\infty(\alpha)>u_{\max}$

Figures 7 and 8 show the graph of the average u_0 vs T relation, i.e., Eq. (37), with T plotted as the independent variable. The dashed parts of the graphs show where either the width function σ [Eq. (36)] is negative or T [Eq. (37)] is negative so the solution is unphysical. Since we know from the $T=0$ calculation at the end of Sec. III that the solution with lower free energy evolves out of $u_{\min}$ as T increases from zero, the top branch of the curve is the important one. Comparison of Fig. 7 with the $\alpha=0$ solution in Fig. 5 shows that the top branch becomes steeper as α increases. At a certain critical value α_c the top branch of the u_0 vs T relation develops an infinite slope, showing the existence of a second-order transition at this single α value; then for larger α values (Fig. 8) the top branch folds back and becomes multivalued, which means that a first-order transition has developed.

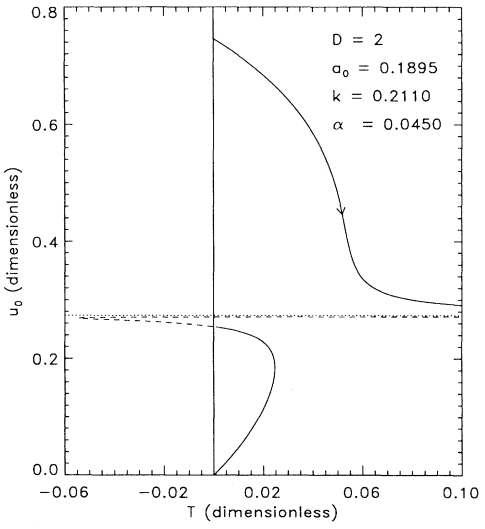

FIG. 7. Average displacement vs temperature, Eq. (37), for the asymmetric on-site potential and for $\alpha=0.045$, which is less than α_c. The dashed part shows the unphysical region where the width function σ [Eq. (36)] is negative, and where Eq. (37) gives a negative T. The dotted line is the high-temperature asymptote $u_\infty(\alpha)$, Eq. (38). The arrow shows the path followed by u_0 for increasing T, starting from $T=0$.

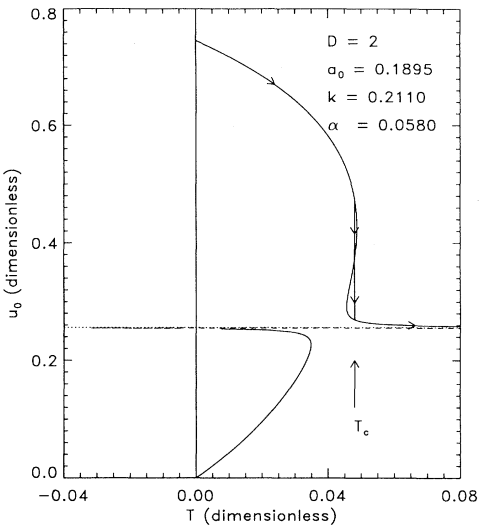

FIG. 8. Average displacement vs temperature, Eq. (37), for the asymmetric on-site potential and for $\alpha=0.058$, which is in the range $\alpha_c<\alpha<\alpha_{s1}$. The dashed part shows the unphysical region where the width function σ [Eq. (36)] is negative, and where Eq. (37) gives a negative T. The dotted line is the high-temperature asymptote $u_\infty(\alpha)$, Eq. (38). The arrow shows T_c, and the vertical line above T_c shows the discontinuity in the average displacement. The arrows on the curves show the path followed by u_0 for increasing T, starting from $T=0$.

The critical value α_c, where the transition first develops, is the value for which the equations

$$\frac{dT}{du_0}=0 , \quad \frac{d^2T}{du_0^2}=0 \tag{42}$$

have a common solution for u_0 in the range $u_\infty(\alpha)<u_0<u_{\min}$.[24] These are simultaneous equations involving sixth-order polynomials, which along with Eq. (37) determine α_c and the values of T and u_0 where the transition initially occurs. We have not obtained an analytic solution of these equations, but if we assign to D, a_0, and k the values used in the simulations[8] (given in the figures), then numerically we find $\alpha_c=0.0537\ldots$, and $T_c(\alpha_c)=0.0502\ldots$.

This scenario of a minimum value for α being required to have a first-order transition qualitatively agrees with the computer simulations; see Fig. 8 of Ref. 8. The critical α found in the simulations (converted to the dimen-

sionless values used here) is $\alpha_c^{(MD)} \approx 0.124$,[25] and the corresponding critical temperature is $T_c^{(MD)}(\alpha_c) \approx 0.031$. Since MFT neglects fluctuations, these relations among the MFT values and the simulation results are reasonable.

For $\alpha > \alpha_c$ there is a discontinuous jump in the average displacement (see Fig. 8) as the temperature increases. Figure 9 shows the free energy per particle, obtained by substituting the solutions for $u_0(T)$ and $\sigma(T)$ into Eq. (20), for $\alpha = 0.058$. Just to the left of the maximum of the solid curve in Fig. 9(a), there is a small "glitch" on the graph. When this part is expanded in Fig. 9(b), we see that it is a loop, analogous to the loop obtained in the free energy of the van der Waals gas.[26] This loop is derived from the part of the top branch of the u_0 vs T relation that folds back. The discontinuous jump in the average displacement (Fig. 8) occurs at the temperature of the intersection point of this loop. Note that above the critical temperature the average displacement continues to decrease toward $u_\infty(\alpha)$. This means that u_0 is not the order parameter in the sense defined by Landau, i.e., a quantity which is identically zero in the high-temperature phase. This situation is again similar to the van der Waals gas.

In Fig. 9(a), the dashed loop on the left is the free energy corresponding to the lower branch of the u_0 vs T relation in Fig. 8, similar to the situation for $\alpha = 0$ in Fig. 6. At each temperature, these values are higher than those from the top branch of the u_0 vs T relation, so it is not the equilibrium solution. The jump in the average displacement occurs between two points on one branch (the upper branch) of Eq. (37).

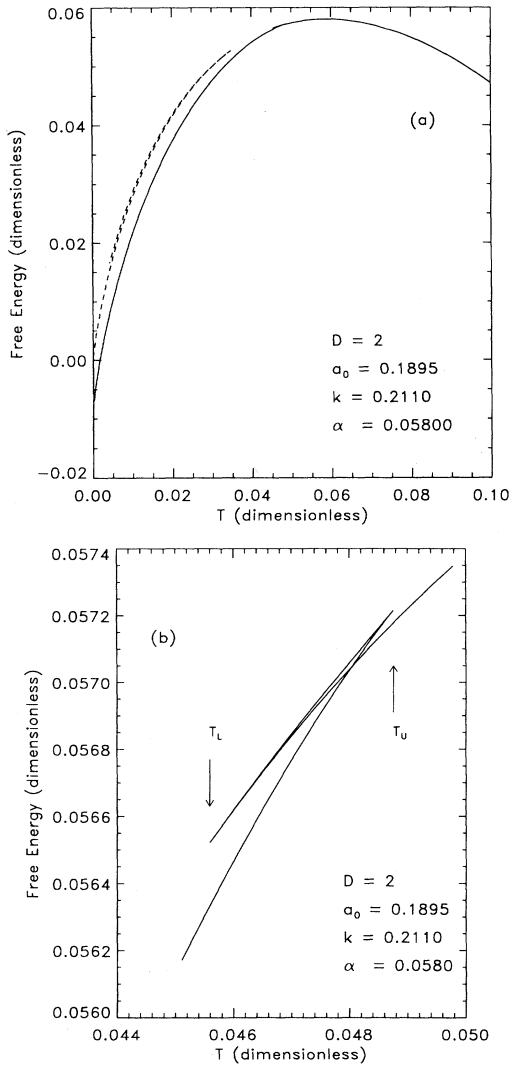

FIG. 9. (a) The free energy for $\alpha = 0.058$, corresponding to the average displacement graph in Fig. 8. The solid curve corresponds to the upper branch of Fig. 8, and the dashed curve is a very narrow loop corresponding to the lower branch. (b) A magnification of part of (a) to the left of the maximum of the solid curve showing the van der Waals loop. T_U and T_L mark the temperature extremes of the loop.

B. $\alpha_{s1} < \alpha < \alpha_{s2}$ or $u_{max} > u_\infty(\alpha) > 0$

For this range of α values, where the high-temperature limiting value of the order parameter $u_\infty(\alpha)$ is less than u_{max}, the u_0 vs T relation takes on the shape shown in Fig. 10 (which is for the value $\alpha = 0.1$). In this case, the upper branch folds back completely to the $T = 0$ axis, whereas the lower branch is monotonically increasing. At $T = 0$, the equilibrium solution for u_0 starts at u_{min} on the upper branch, just as in the previous subsection, and then it jumps to the lower branch at the temperature where the free energies of these two branches become

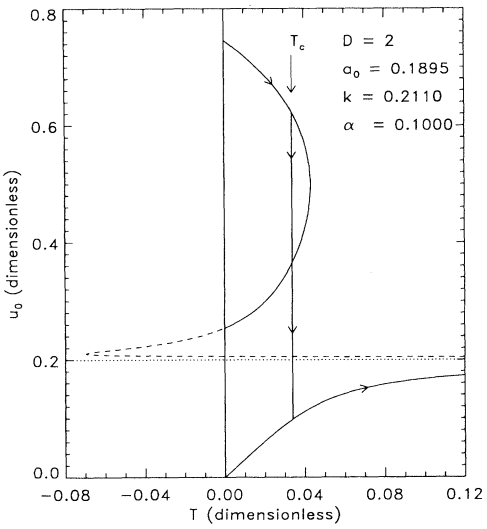

FIG. 10. Average displacement vs temperature, Eq. (37), for the asymmetric on-site potential, and for $\alpha = 0.1$, which is in the range $\alpha_{s1} < \alpha < \alpha_{s2}$. The dotted part shows the unphysical region where the width function σ [Eq. (36)] is negative, and where Eq. (37) gives a negative T. The dotted line is the high-temperature asymptote $u_\infty(\alpha)$, Eq. (38). The arrow shows T_c, and the vertical line below the arrow shows the discontinuity in the average displacement. The arrows on the curves show the path followed by u_0 for increasing T, starting from $T = 0$.

equal. The free energy for this situation is shown in Fig. 11. The part arising from the upper branch of the u_0 vs T relation folds sharply back. The equilibrium solution starts out on the lower part of this branch, and then switches to the other branch at the temperature where the two branches cross. There is no *closed* loop in either branch of the free-energy graph in this case, as there was in the previous subsection. There are two further contrasts to the behavior in the previous subsection: (i) the order parameter jumps between the two *different* branches of the u_0 vs T relation, and (ii) above the critical temperature the average displacement *increases* toward $u_\infty(\alpha)$.

C. $\alpha > \alpha_{s2}$ or $0 > u_\infty(\alpha)$

When α is made larger than $\alpha_{s2}=1/2D$, then $u_\infty(\alpha)$, the high-temperature asymptote of the average displacement, becomes negative [Eq. (38)]. A plot of the u_0 vs T relation for an α value in this range is shown in Fig. 12. At the transition, the average displacement jumps from a position in the stable well of the on-site potential to a position on the *left* of its metastable minimum. The on-site potential energy can be large at such a position (see Fig. 1), but the average of the interaction potential energy, Eq. (17), is reduced and can become negative for sufficiently large and negative u_0, because of the factor $(k+2\alpha u_0)$. We note that in this situation the jump in the average displacement again occurs between two points on the same branch of the u_0 vs T relation, and that u_0 decreases towards $u_\infty(\alpha)$ above the transition, as in Sec. V A above.

In Ref. 8 an exact stability analysis at $T=0$ showed that for sufficiently large α, the lowest-energy configuration has the lattice divided into two interpenetrating sublattices with opposite displacements of unequal magnitude on the two sublattices.[27] Such a configuration cannot be described by our spatially uniform Gaussian ansatz in Eq. (9) for the position probability distribution. For the values of D, a_0, and k used in the simulations, the two-sublattice solution becomes the minimum energy solution at $\alpha=0.509\ldots$.[28] This value of α is then the upper limit of applicability for the formulation of MFT in Sec. III.

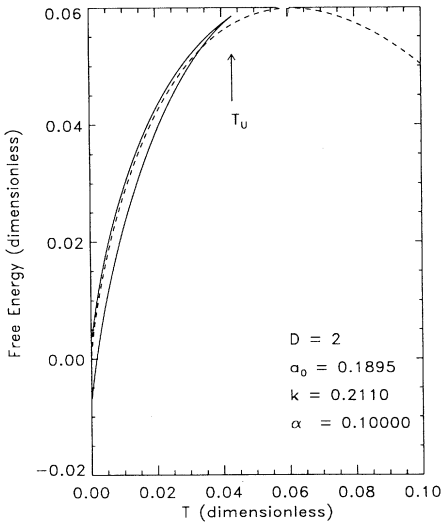

FIG. 11. The free energy for $\alpha=0.1$, corresponding to the average displacement graph shown in Fig. 10. The solid curve corresponds to the upper branch of Fig. 10, and the dashed curve to the lower branch. T_U marks the highest temperature of the curve shown with the solid line.

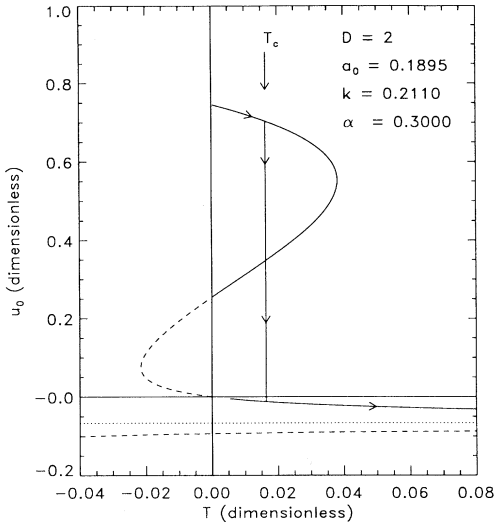

FIG. 12. Average displacement vs temperature, Eq. (37), for $\alpha=0.30$. The dashed part shows the unphysical region where the width function σ [Eq. (36)] is negative, and where Eq. (37) gives a negative T. The dotted line is the high-temperature asymptote $u_\infty(\alpha)$, Eq. (38). The arrow shows T_c, and the vertical line below the arrow shows the discontinuity in the average displacement. The arrows on the curves show the path followed by u_0 for increasing T, starting from $T=0$.

The MFT solutions, Eqs. (36) and (37), predict the u_0 vs T relation changes shape again at $\alpha\approx 0.9075\ldots$ (which depends on the values of a_0, D, and k). The cubic polynomial in the curly brackets in Eq. (37) has a single real root up to this value and develops three real roots beyond it. The mean-field critical temperature T_c decreases to zero as α increases to this value. Thus, the MFT equations themselves indicate the Gaussian ansatz fails at an α value which is about twice as large as given by the exact analysis.

D. Summary of this section

In the previous subsections we showed that sufficiently strong anharmonicity in the interparticle interactions causes a first-order transition to occur in this system. We further showed that increases in the strength of this anharmonicity cause changes in the shape of the average displacement vs temperature relation at certain "crossover" values. In Fig. 13 we show the dependence of T_c on the anharmonicity strength over the whole range of values, along with the results from the MD simulations.[29] There is a horizontal shift of the MFT results relative to the simulations, i.e., the critical value of α according to

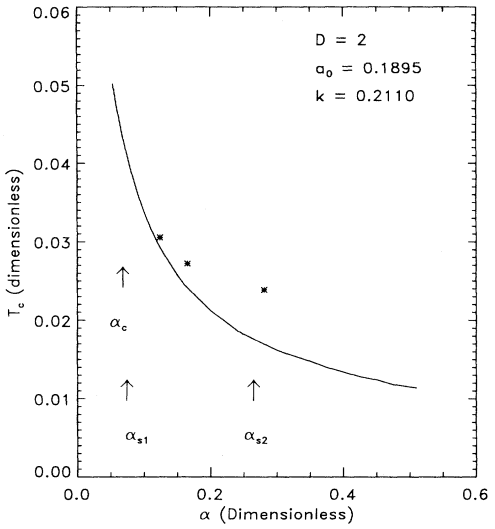

FIG. 13. The variation of the critical temperature with the strength of the anharmonicity parameter α. The MFT values for the minimum value to have a transition and the two "switchover" values are marked. The maximum value of α plotted is the stability limit found in Ref. 8 for the ground state displacement pattern to remain uniform. The three points show the results from the MD calculations.

the MD is about $\alpha_c \approx 0.124$ (the MD point at the smallest α), whereas the MFT gives $\alpha_c = 0.0537\ldots$. The decrease in T_c with increasing α is understandable from the assertion that this transition is entropy driven; increasing the anharmonicity strength allows the disordering effect to occur at a lower temperature. The largest α value plotted is where the exact $T=0$ analysis shows that nonuniform displacements develop on different sublattices. The MFT equations would allow the graph to continue on to $\alpha = 0.9075$.

For α in the range $\alpha_c < \alpha < \alpha_{s1}$, we noted in Sec. V A above that the jump in the average displacement takes place on one branch of the u_0 vs T relation, and in Sec. V B we found that for $\alpha_{s1} < \alpha < \alpha_{s2}$, the jump is between the two different branches of that relation. Furthermore, for the range of smaller α values, u_0 continues to *decrease* toward $u_\infty(\alpha)$ for increasing temperature above T_c. Conversely, for the range of intermediate α values, u_0 *increases* toward $u_\infty(\alpha)$ for increasing temperature above T_c. This feature of having different ranges of α values is also present in the computer simulations; Fig. 8 of Ref. 8 shows the average displacement *decreasing* toward the high-temperature limit for smaller α values, and *increasing* toward that limit for larger α values. The value $\alpha = 0.281$ (Ref. 30) used for most of the simulations in Ref. 8 was evidently in the intermediate α range and close to its upper limit, since the values of u_0 are increasing slowly above T_c. According to the MFT, the value $\alpha = 0.281$ is in the *third* range of α values, where the average displacement should be negative (Secs. V C above). Thus, the MFT predictions of the boundaries between the different α ranges are not exact. The existence of the different α ranges was not known when those simulations were done, so no MD determination of the "switchover" values was made.

It is important to note that in the range of smaller α values (Sec. V A) where the high-temperature limit $u_\infty(\alpha)$ of the order parameter is larger than $u_{\max}$, the jump in the average displacement at the transition takes place between two values which are both in the deeper well of the on-site potential (see Fig. 1). For the ranges of larger α values (Secs. V B and V C), the average displacement jumps between a low-temperature value in the stable well and a high-temperature value in the metastable well. For all rangles of α, increasing the temperature above T_c moves u_0 away from the nearby minimum of the on-site potential, which costs internal energy. The occurrence of this transition must be due to the gain in entropy associated with it.

We can compute the entropy from the free energy, since $s = -df/dT$. The total temperature dependence of the free energy in Eq. (20) is obtained by substituting the solutions of Eqs. (21) and (22) before doing the differentiation. Thus,

$$s = -\left[\frac{\partial f}{\partial T}\right] - \left[\frac{\partial f}{\partial u_0}\right]\Bigg|_{u_0(T),\sigma(T)} \frac{du_0}{dT} - \left[\frac{\partial f}{\partial \sigma}\right]\Bigg|_{u_0(T),\sigma(T)} \frac{d\sigma}{dT} . \tag{43}$$

The quantities $\partial f/\partial u_0$ and $\partial f/\partial \sigma$ vanish when evaluated for the solutions u_0 and σ because those are just the MFT equations, Eqs. (21) and (22). Thus, the entropy is given by the differentiation of just the explicit dependence of f on T, which is Eq. (19). The results are shown in Fig. 14, for an α value in each of the three ranges. On the overall scale of variation of the entropy, the size of

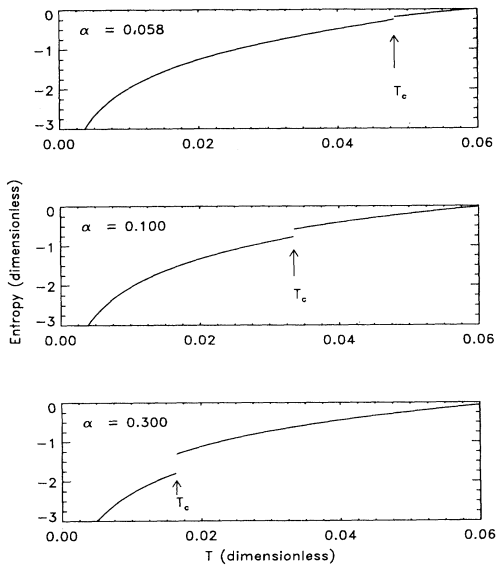

FIG. 14. Entropy per particle vs temperature for three different α values, one in each of the different ranges. The arrows mark the corresponding critical temperature.

the discontinuity associated with the transition seems rather small. However, it must be the effect driving the transition.

We conclude this section with a more speculative connection between the MD results and this MFT. The most extensive simulations in Ref. 8 were done for an α value in the intermediate range, and they exhibited hysteresis. In fact, a transition was obtained only on heating the system and was never seen on cooling. Subsequent simulations using a constant temperature method[31] (in contrast to the constant energy method of Ref. 8) have the same hysteresis in the intermediate α range; they do not have it, or have it over a much smaller temperature interval in the small α range. This effect can be understood from the results for the free energy in Figs. 9(b) and 14. In the small α range the free energy has a "van der Waals" loop in it, and the temperatures at the ends of that loop [marked T_U and T_L on Fig. 9(b)] are the (mean-field) stability limits of the system. A system in the low-temperature phase can be heated no higher than T_U, nor one starting in the high-temperature phase cooled no lower than T_L before a transition takes place. The range on the T axis in Fig. 9(b) show that these temperatures are, in fact, rather close together. In contrast since there is no closed loop in the free-energy curves for the intermediate α range (Fig. 11), there is a stability limit at T_U only on heating the system. A system being cooled from the high-temperature phase can be taken all the way down to $T=0$ with the average displacement following the lower branch in Fig. 10 into the metastable minimum of the on-site potential. This is the qualitative behavior shown by the simulations.

VI. CONCLUSIONS

In this paper we have constructed an approximate theory for a lattice dynamical model which exhibits a first-order structural phase transition. The essential features of the model are (i) it has a one-component order parameter, placing it in the Ising universality class; (ii) each particle moves in an asymmetric on-site potential; and (iii) anharmonicity is included in the interparticle interaction. The asymmetry of the on-site potential precludes a symmetry-breaking transition; in fact, if only features (i) and (ii) are present, no transition occurs. The third feature, i.e., the anharmonicity of the interactions, makes the lattice vibrational frequencies dependent on the structure. This dependence provides a mechanism which increases the entropy of the high-energy structure relative to the low-energy structure, and thereby achieves a lower free energy at higher temperatures. Thus, this model demonstrates a transition which it totally *entropy driven*, and for which symmetry breaking plays no role.

The theory is based on the mean-field assumption that the particles move independently of each other, and further assumes that the single-particle probability distribution is Gaussian. The results show that there is a minimum strength of interparticle anharmonicity necessary to have a transition, and further shows that there are several different intervals of anharmonicity strength within which the average displacement vs temperature relation has different shape. This theory and the computer simulations on the model qualitatively agree in the parameter regions where they overlap, and the theory has shown existence of other parameter regions not covered in the original simulations. The theory provides an explanation for the hysteresis seen in the simulations.

ACKNOWLEDGMENTS

The authors wish to thank Professor Dilip Kondepudi for an insight which led to an important improvement in this work. The computer simulations reported in Ref. 8, which motivated this work, were supported by NSF Grant No. CHE-8913800 to Wake Forest University.

*Present address: Carteret Community College, 3505 Arendell St., Moorehead City, NC 28557-2989.

[1]W. Cochran, Adv. Phys. **9**, 387 (1960).

[2]P. W. Anderson, in *Fizika Dielectrikov,* edited by G. I. Skanov and K. V. Fillippov (Academy of Sciences, Moscow, 1960), p. 290.

[3]K. A. Müller and W. Berlinger, Phys. Rev. Lett. **26**, 13 (1971).

[4]T. Riste, E. J. Samuelson, K. Otnes, and J. Feder, Solid State Commun. **9**, 1455 (1971); S. M. Shapiro, J. D. Axe, G. Shirane, and T. Riste, Phys. Rev. B **6**, 4332 (1972).

[5]J. A. Krumhansl, in *Competing Interactions and Microstructures,* edited by R. LeSar, A. R. Bishop, and R. Heffner (Springer, New York, 1988), p. 50.

[6]J. A. Krumhansl and R. J. Gooding, Phys. Rev. B **39**, 3047 (1989).

[7]S. M. Shapiro, B. X. Yang, G. Shirane, Y. Noda, and L. E. Tanner, Phys. Rev. Lett. **62**, 1298 (1989); A. Heiming, W. Petry, J. Trampenau, M. Alba, C. Herzig, and G. Vogl, Phys. Rev. B **40**, 11 425 (1989); W. Petry, A. Heiming, J. Trampenau, M. Alba, C. Herzig, H. R. Schober, and G. Vogl, *ibid.* **43**, 10 933 (1991); A. Heiming, W. Petry, J. Trampenau, M. Alba, C. Herzig, H. R. Schober, and G. Vogl, *ibid.* **43**, 10 948 (1991); J. Trampenau, A. Heiming, W. Petry, M. Alba, C. Herzig, W. Miekeley, and H. R. Schober, *ibid.* **43**, 10 963 (1991).

[8]W. C. Kerr, A. M. Hawthorne, R. J. Gooding, A. R. Bishop, and J. A. Krumhansl, Phys. Rev. B **45**, 7036 (1992).

[9]J. R. Morris and R. J. Gooding, Phys. Rev. Lett. **65**, 1769 (1990); R. J. Gooding, Scr. Met. **25**, 105 (1991); J. R. Morris and R. J. Gooding, Phys. Rev. B **43**, 6057 (1991); **46**, 8733 (1992); J. Stat. Phys. **67**, 471 (1992); R. J. Gooding and J. R. Morris, Phys. Rev. E **47**, 2134 (1993).

[10]T. Dauxois, M. Peyrard, and A. R. Bishop, Phys. Rev. E **47**, R44 (1993).

[11]A. D. Bruce, Adv. Phys. **9**, 111 (1980).

[12]H. Thomas, in *Structural Phase Transitions and Soft Modes,* edited by E. Samuelson, E. Anderson, and J. Feder (Oslo, Universitetsforlaget, 1971).

[13]E. K. H. Salje, B. Wruck, and H. Thomas, Z. Phys. B **82**, 399 (1991).

[14]C. Zener, Phys. Rev. **71**, 846 (1947).

[15]R. A. Cowley, Adv. Phys. **29**, 1 (1980), see Sec. I.4.3.2, and

references therein.
[16]G. Parisi, *Statistical Field Theory* (Addison-Wesley, Redwood City, 1988), p. 24.
[17]See Figs. 14 and 15 of Ref. 8.
[18]M. J. Rave and W. C. Kerr (unpublished).
[19]This is the solution if $(2Dk/3-\frac{1}{27})>0$. Otherwise, one must choose the other sign in the quadratic formula. The result gives only negative values for σ, which is unphysical.
[20]W. C. Kerr and A. R. Bishop, Phys. Rev. B **34**, 6295 (1986).
[21]Conversion between the different dimensionless variables used in these two papers has to be done to make this comparison.
[22]See, e.g., K. Huang, *Statistical Mechanics* (Wiley, New York, 1980), pp. 428–432.
[23]R. Brout, K. A. Müller, and H. Thomas, Solid State Commun. **4**, 507 (1966); A. D. Bruce, in *Solitons and Condensed Matter Physics,* edited by A. R. Bishop and T. Schneider (Springer, New York, 1978), p. 116; A. D. Bruce, T. Schneider, and E. Stoll, Phys. Rev. Lett. **43**, 1284 (1979).
[24]This situation is analogous to the calculation of the critical point for the van der Waals gas.
[25]This is value $\alpha_c=1.50$ eV/Å^3 found in the simulations.
[26]C. Kittel and H. Kroemer, *Thermal Physics* (Freeman, San Francisco, 1980), p. 293.
[27]See end of Sec. II of Ref. 8.
[28]This is the value $\alpha=6.16$ eV/Å^3.
[29]The MD results show the T_c values obtained for *heating* the system. Considerable hysteresis existed in the simulations for heating and cooling. See Ref. 8.
[30]This is the value $\alpha=3.40$ eV/Å^3.
[31]W. C. Kerr, P. S. Lomdahl, and D. M. Beazley (unpublished).